Lawrence Berkeley Laboratory
UNIVERSITY OF CALIFORNIA
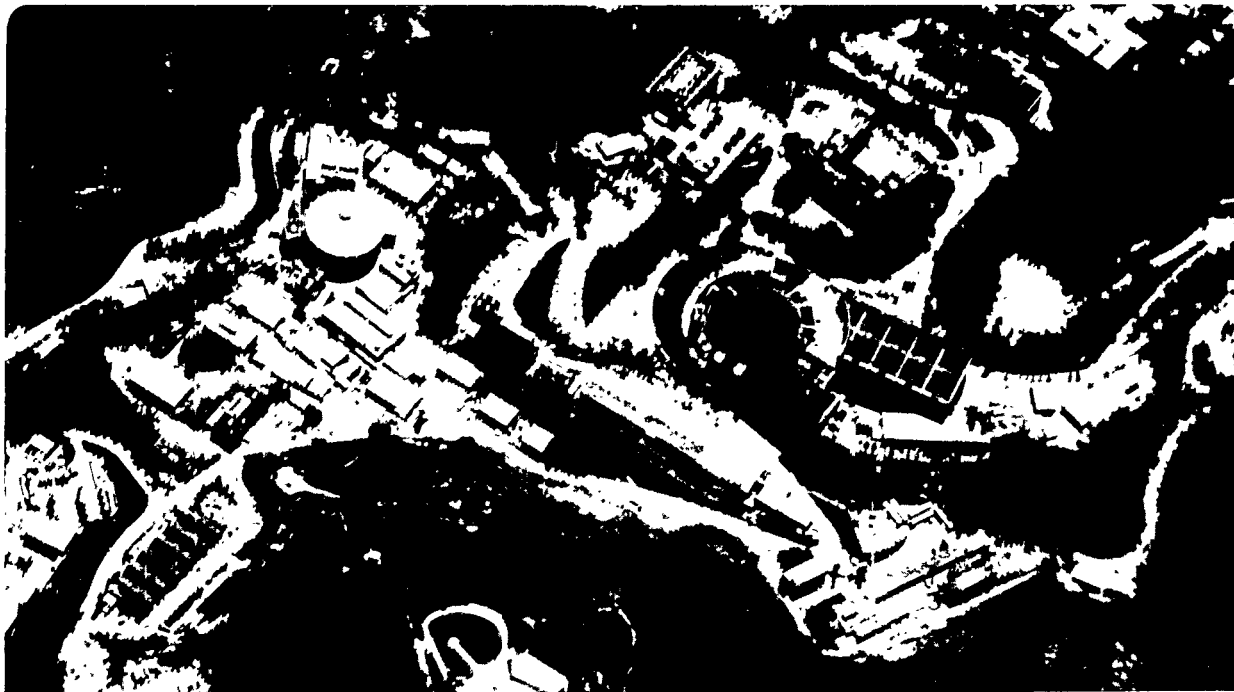
Physics Division

Detection of Charged Particles and X-Rays by Scintillator Layers Coupled to Amorphous Silicon Photodiode Arrays

T. Jing, C.A. Goodman, J. Drewery, W.S. Hong, H. Lee,
S.N. Kaplan, V. Perez-Mendez, and D. Wildermuth

April 1995

DISCLAIMER

DISCLAIMER

Portions of this document may be illegible in electronic image products. Images are produced from the best available original document.

Detection of charged particles and X-rays by scintillator layers coupled to amorphous silicon photodiode arrays

T. Jing, C. A. Goodman* , J. Drewery, W.S. Hong, H. Lee, S. N. Kaplan, V.

Perez-Mendez, D. Wildermuth*

Physics Division

Lawrence Berkeley Laboratory

Berkeley, CA 94720

* Air Techniques, Inc. Hicksville, NY11802

April 1995

.

Detection of charged particles and X-rays by scintillator layers coupled to amorphous silicon photodiode arrays

T. Jing, C. A. Goodman*, J. Drewery, G. Cho, W.S. Hong, H. Lee, S. N. Kaplan, V. Perez-Mendez, D. Wildermuth*

Lawrence Berkeley Laboratory

Berkeley, CA 94720

* Air Techniques, Inc. Hicksville, NY11802

ABSTRACT

Hydrogenated amorphous silicon (a-Si:H) p-i-n diodes with transparent metallic contacts are shown to be suitable for detecting charged particles, electrons, and X-rays. When coupled to a suitable scintillator using CsI(Tl) as the scintillator we show a capability to detect minimum ionizing particles with S/N ~20. We demonstrate such an arrangement by operating a p-i-n diode in photovolaic mode (reverse bias). Moreover, we show that a p-i-n diode can also work as a photoconductor under forward bias and produces a gain yield of 3-8 higher light sensitivity for shaping times of 1 μs. n-i-n devices have similar optical gain as the p-i-n photoconductor for short integrating times (< 10μs). However, n-i-n devices exhibit much higher gain for a long term integration (10ms) than the p-i-n ones. High sensitivity photosensors are very desirable for X-ray medical imaging because radiation exposure dose can be reduced significantly. The scintillator CsI layers we made have higher spatial resolution than the Kodak commercial scintillator screens due to their internal columnar structure which can collimate the scintillation light. Evaporated CsI layers are shown to be more resistant to radiation damage than the crystalline bulk CsI(Tl).

1. Introduction

Hydrogenated amorphous silicon (a-Si:H) p-i-n photodiodes with transparent metallic contacts are widely used as solar cells due to their ease of deposition in large areas at low cost. Since amorphous silicon is a direct band gap material, the thickness necessary to detect visible light is < 1µm[1]. A high Z scintillator layer coupled to an a-Si:H pixel array therefore can serve as a position sensitive detector for Minimum Ionizing Particles-MIPs as well as for X-rays.

In this paper we describe the use of Thallium activated Cesium iodide layers 50-1000µm thick evaporated on to a-Si:H p-i-n pixel or strip arrays with transparent Indium Tin Oxide-ITO contacts. We picked CsI(Tl) as the scintillator of choice because it produces the largest amount of light (> 50,000 visible light photons/ MeV of deposited energy) of any high Z scintillator[2]. It has other desirable properties such as moderate hygroscopity and as we have shown previously[3] can be evaporated to form thin columns which tend to collimate its light output and hence produce a good spatial resolution.

We also show how moderate, stable, photoconductive gain can be obtained by operating the p-i-n photodiode under a forward bias, or by using an n-i-n configuration. In this paper, we demonstrate the detection of minimum ionizing particles - electrons and X-rays using a radiation detector based on a CsI scintillator layer coupled to a-Si:H photosensor.

2. Photosensor operating characteristics

2.1. a-Si:H pin diode

A p-i-n structure is used for the photodiode with a transparent ITO-Indium Tin Oxide conducting layer coating on top. The amorphous layer was deposited on a glass substrate coated with a Cr layer. The p^+ blocking layer was thin ~ 10nm in order not to lose conversion electrons in it.. The i-layer thickness varies between 0.5 and 1 µm for light detection in the photovoltic mode. However, for our detectors we sometimes used 10-14 µm thick p-i-n diodes in order to reduce the capacity thus decreasing the noise level from the preamplifier.
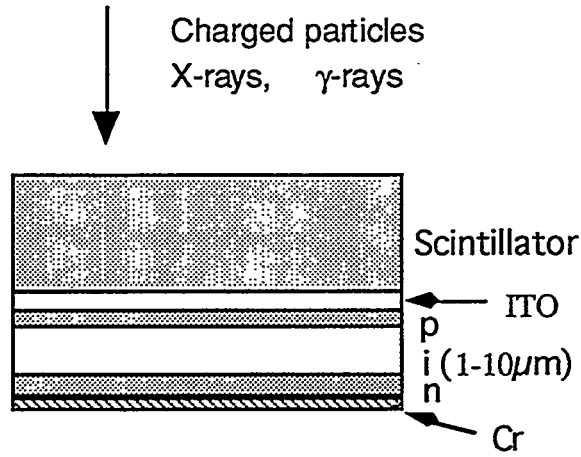
Fig.1 Schematic of CsI(Tl)/a-Si:H detector configuration.

2.2. Charge collection efficiency

Since the scintillation light wavelength emitted from CsI(Tl) is less than 650nm and peaks at 560nm with mean free path ~ 0.3 μm in the i layer[4], it will be strongly absorbed within a short distance when it is incident on the amorphous silicon. When the scintillation light is incident on the p-side of a 10 μm thick a-Si:H p-i-n detector, the signal is induced primarily by the electrons, because the transit distance of the holes to the contact is short compared to the electron transit.
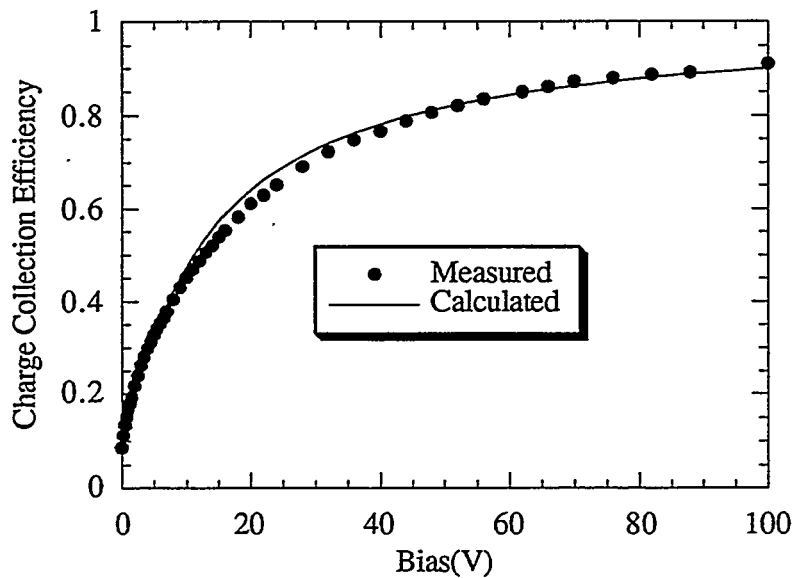

Fig.2.(a) Charge collection efficiency for various bias voltagefor a 10 μm thick diode.
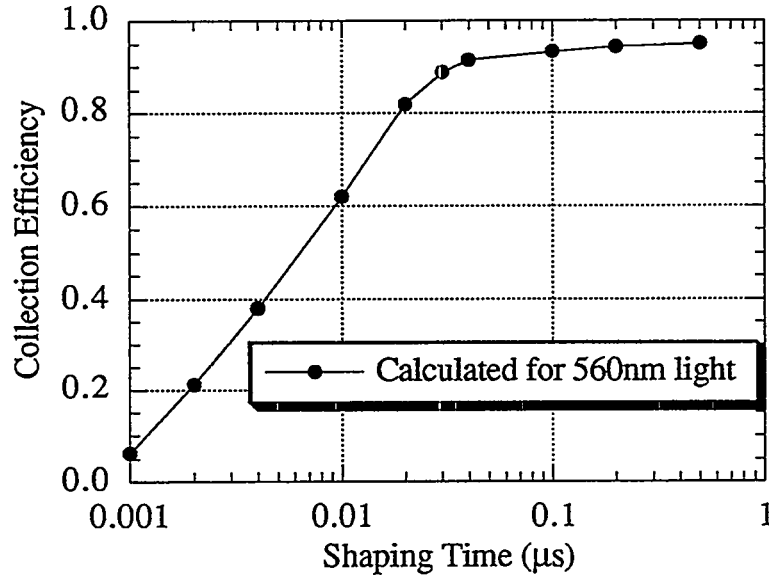
3

Fig.2 (b) Collection efficiency for different shaping times for 560nm light on a 10 μm diode.

The signal size dependence of the shaping time was measured by exposing a short light pulse(200 ns) with wavelength 560 nm from the p side of the diode to simulate the scintillation light from CsI(Tl). The operating bias was set at - 100 volts on a 10 μm thick p-i-n diode. For this wave length light, only one type of carrier involves the signal formation as noted, therefore, the signal measured by the external circuit is virtually all due to the collection of the electrons. For a p-i-n diode with 10 μm thick i layer the transit time of the electrons at a bias of 100V is less than 15ns.

The measured and calculated charge collection efficiency for 10 μm thick p-i-n diodes is shown in Fig.2(a). Fig.2(b) shows the charge collection efficiency as a function of RC-CR shaping time.

A typical spectral dependence of the charge collection,$Q(\lambda)$, of a p-i-n device is shown in Fig.3; this reaches its peak value of 80% at wavelengths between 500-600nm, indicating that there is little loss due to recombination.
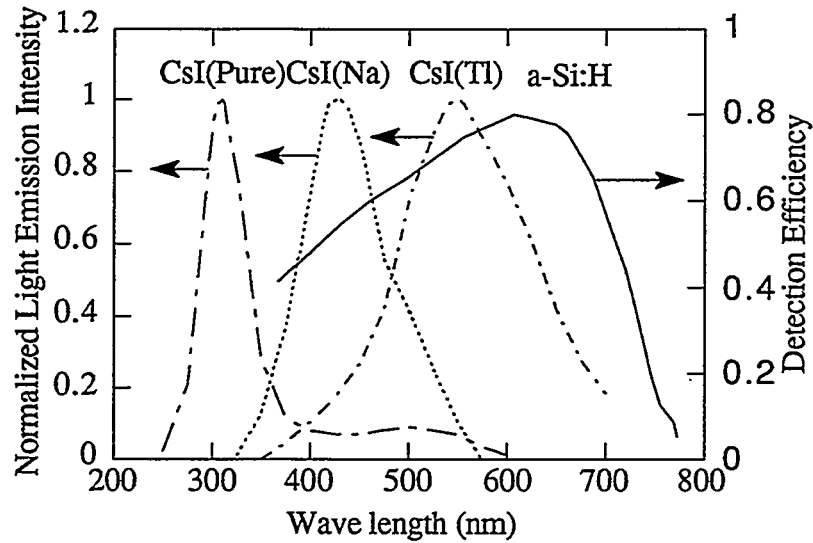
4

Fig.3 Scintillation light spectra of CsI(Tl) and CsI(Na) and detection efficiency
of a-Si:H photodiodes.

The decreased collection efficiency at short wavelengthes has several origins. One cause is the absorption of light in the p or n layer, whichever is directly exposed to the incident light. The resulting carriers give virtually no contribution to the charge collection because of the relatively low minority carrier lifetime in the doped layers, since most of the light absorbed in the doped layer is lost to recombination[5]. The thickness of the p layer must be optimized; thin enough to minimize the light absorption and thick enough to prevent tunneling across the p-i junction and breakdown. A p-type a-SiC:H alloy layer is used for higher collection efficiency, because a-SiC:H has a wider band gap from 1.9 to 2.3 eV depending on the content of the carbon[6], hence has a lower absorption than a p-doped a-Si:H layer.

2.3 Addressed pixel signal readout

Signal acquision of a sensor array is normally performed in a charge storage mode. The photogenerated charge or the light-induced voltage across the diode capacitance at the end of the line-scan time is transferred to the output by switching on the corresponding multiplexing switch. Such addressing switches can be made using single diode, two diode, or thin film transistors (TFT)[7-9]. Single diode readouts have the simplest processing steps, however, the feed-

through transient charges from the addressing pulse may affect the signal-to-noise ratio. A modification of the fundamental scheme has been developed[10], using two diodes per pixel to cancel the transient; this has the advantage of smaller transients, higher linearity and higher readout speed. a-Si:H or poly-Si TFTs have been successfully used as readout switches. These various readout scheme have been described elsewhere[7-12].

3. Scintillator

3.1. CsI(Tl) layer fabrication

It is well known that dopant thallium atoms in alkali halide scintillators work as activators which play an important role in increasing the scintillation efficiency and in producing a longer wavelength emission spectrum than CsI(Na). This is a better match to the a-Si:H detector as shown in Fig.3. A homogeneous concentration of the Tl is necessary in order to optimize the performance of the CsI(Tl) scintillator. The conventional evaporation techniques do not produce deposits having the same composition as the source material when the vapor pressures of the constituents TlI and CsI in the evaporation boat are dramatically different. The CsI(Tl) layers produced by this method have large gradients in Tl concentration. To avoid this problem we adopted a powder flash evaporation technique[13]. The setup of the evaporator we used is shown schematically in Fig.4. The source material is a powder mixture of CsI and TlI according to the predetermined Tl concentration. The CsI and TlI powder is pressed into pellets and then transported through a tube by a controllable motor and continuously fed into the heated boat. The boat is hot enough to ensure that the mixture vaporizes rapidly. The deposition rate is determined by the feeding speed which is controlled by the motor. The substrates were placed on a rotating holder which was cooled by a water tubing system to maintain the substrates at 100-150 C^0 during the evaporating process. The chamber initially was pumped down to 10^{-6} Torr. An inert gas, in this case, Ar, was then admitted into the chamber which was then maintained at about 5m Torr during the process. Ar atoms modify the transport paths of the vapor toward the substrate by scattering, which

6

enhances the columnar structure of the CsI layers, thus improving the spatial resolution of the detector. A typical morphology of the evaporated CsI(Tl) layer is shown in Fig.5.
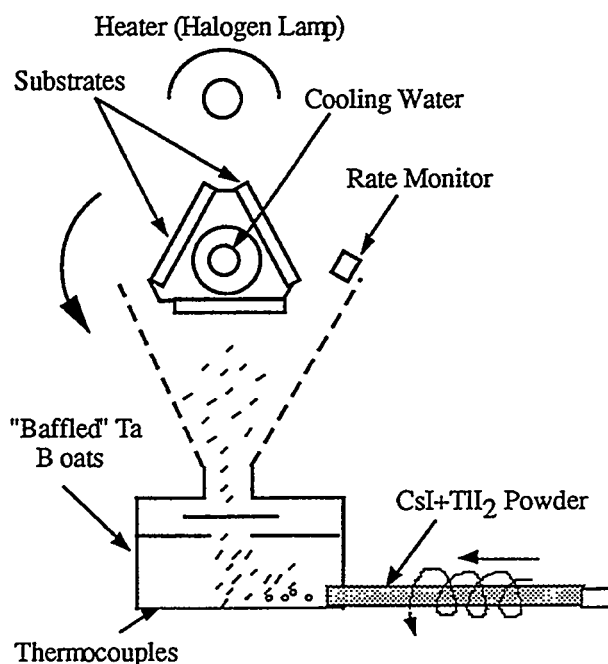

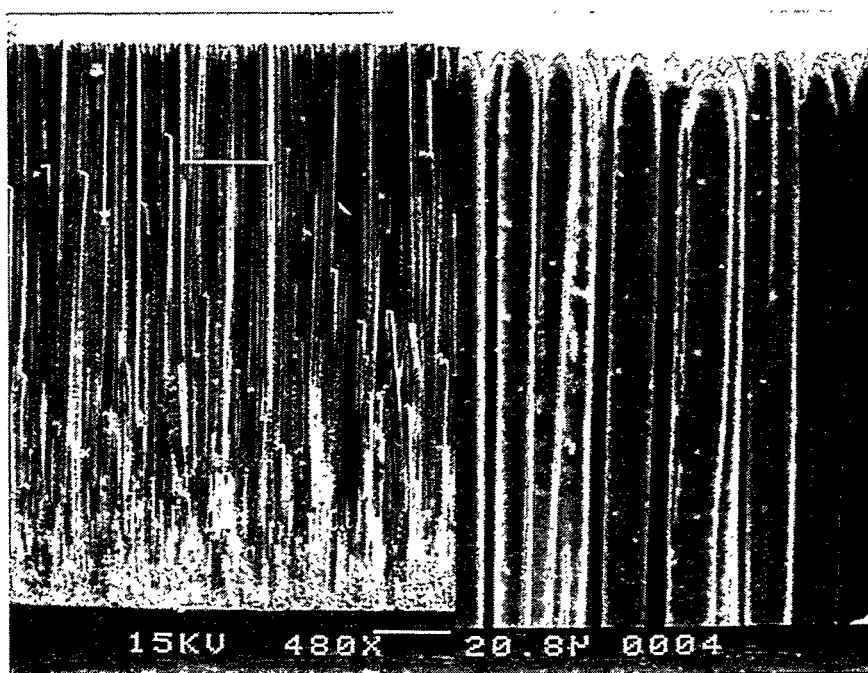Fig. 4 Schematic of setup for depositing CsI(Tl) layers.

Fig.5 SEM of the microstructure of columnar CsI(Tl) layer.

3.2. Timing spectra

CsI(Tl) layers with different Tl concentrations have the same three decay components as the crystal materials, 900ns, 1500ns, and 3500ns[14]. The 900ns component dominates the total light emission.
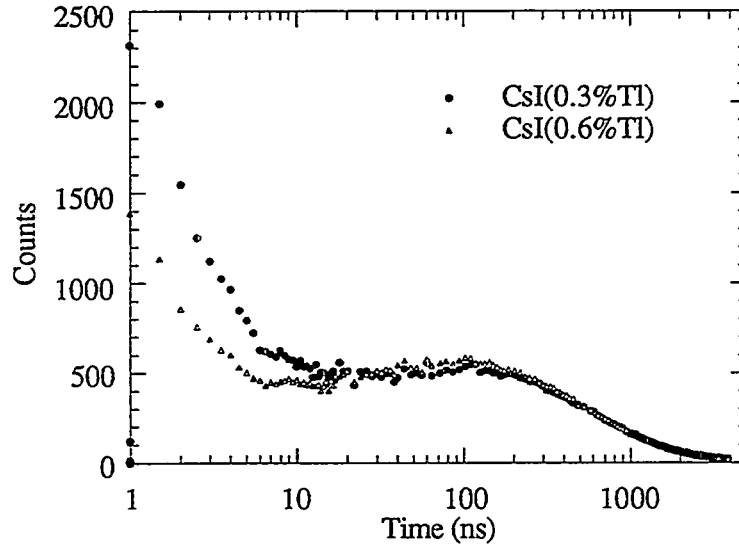

Fig.6 Measured light emission as function of time from evaporated CsI(Tl) layers.

In some applications, such as in particle and nuclear physics, the detector needs to have a fast response to incident events. Normally, the light decay from the scintillator limits the response time in the scintillator/photosensor detector system. The measured timing spectrum from CsI(Tl) evaporated layers is shown in Fig.6. A faster response can be obtained using pure CsI(light decay ~ 10 ns). However its light yield is < 16,000 photos/MeV. A better scintillator for this purpose is Cerium-doped Lutetium Oxyorthosilicate (LSO)[15], which has a fast decay time < 50 ns and a fairly high light emission ~50% of CsI(Tl)[16].

3.3 The effect of the heat treatment

The heat treatment of the CsI layer, not only changes its morphological structure but also affects the light emission efficiency. CsI samples were annealed at temperatures of 200°C to 500°C for 30 minutes. The light output systematically increases with increasing the annealing

temperature. As seen in Fig.7, the initial annealing (from 150°C to 250°C) causes a larger increase in the light yield than the higher temperature annealing. This light output effect of the heat treatment indicates that the annealing can cause the Tl atoms to relocate in the CsI by thermal diffusion processes, which therefore create more Tl$^+$ luminescent centers and thus more effectively activate the CsI to emit the light. In addition, it should be emphasized that at the temperatures beyond 550°C the annealing will degrade the CsI light yield because some of Tl atoms will escape from CsI surface due to the high equilibrium vapor pressure of the TlI.
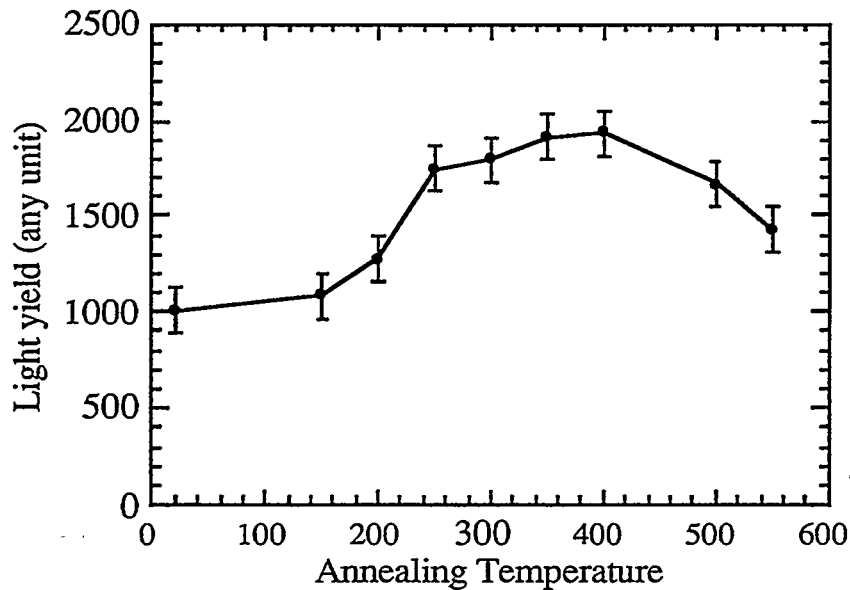

Fig. 7 Light yield vs annealing temperature

3.4. Radiation damage resistance

A scintillation screen, as the input radiation converter, absorbs most of the incoming radiation energy during high rate particle detection or long term medical imaging. It will undergo radiation damage, thereby decreasing the light yield. We have previously shown that the a-Si:H is very resistive to radiation damage[17]. Thus there is concern over the sensitivity of the CsI(Tl) film which may limit its use in high flux radiation detection applications. Previous data[18,19] has

9

shown that the pulse height reduction from bulk crystal CsI(Tl) is already significant at a dose level of 1Gy. We exposed an evaporated CsI(Tl) layer 125 μm thick to various dose levels to determine its radiation tolerance.
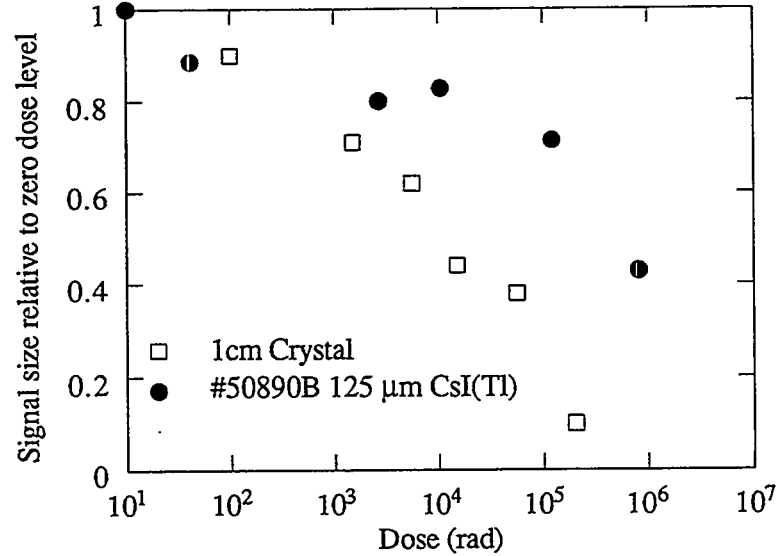

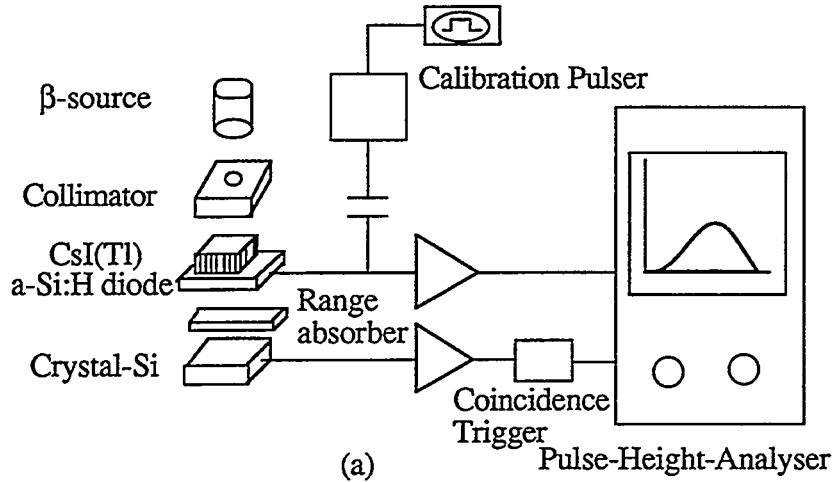Fig.8 Comparison of evaporated CsI layer and crystalline bulk CsI to radiation resistance.

The irradiation was done with a strong γ-ray Co-60 source at the irradiation facility at LBL. The nominal activity of the C0-60 source was 6000 Ci. The CsI(Tl) sample was placed at calibrated positions 10-30 cm away from Co-60 source. An ion chamber detector was used to monitor the dose which determined the exposure time required for the total dose. The signal yield was measured after each exposure. It was normalized relative to its original signal output. Fig.8 shows the data for a 1cm thick crystal CsI(Tl) taken from ref[20] as well as from the evaporated layer.

As shown in Fig. 8, the dose required to reduce the signal size by a factor of two for this evaporated layer is about 50 times larger than that for 1 cm thick bulk crystalline CsI sample. This suggests that the radiation damage changed the optical transmission properties of the scintillator, in agreement with more detailed studies on crystal CsI[20].

10

4. Radiation detection

4.1. ß particle detection

We measured signals produced by minimum-ionizing electrons from a Sr^{90} source with the CsI/a-Si:H pin diode detector. A 10 μm thick a-Si:H pin was used to decrease the detector capacity in order to reduce the noise level of the output. A 950μm thick evaporated CsI(Tl) layer was coupled to a-Si:H photodiode. A thin aluminum foil was placed on the top of the scintillator as reflector to increase light collection. The measurement setup is shown in Fig.9(a). The ß particles were collimated by a 8mm thick aluminum collimator with 1.5 mm diameter hole. A Hamamatsu photodiode S3590-01 was set below the CsI/a-Si;H pin detector as a trigger counter to count only the high energy > 1.5 MeV tail of the beta spectrum. The output of the photodiode was amplified by a charge-sensitive amplifier and then connected through a shaping amplifier to a PHA. The shaping time was set at 1 μs.

(a)

A typical pulse-height distribution for the measurement is shown in fig.9(b). The peak of the spectra corresponds to approximately 22,000 electron-hole pairs. This is equivalent to a generated light yield of 40,000 visible scintillation photons[21]. This signal size can be increased by a factor ~ 3-6 using the photoconductivity gain mechanism discussed in section 5.
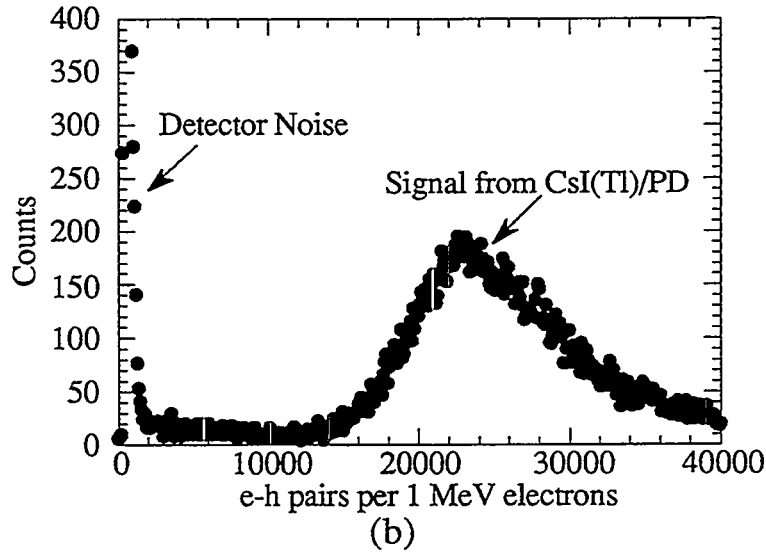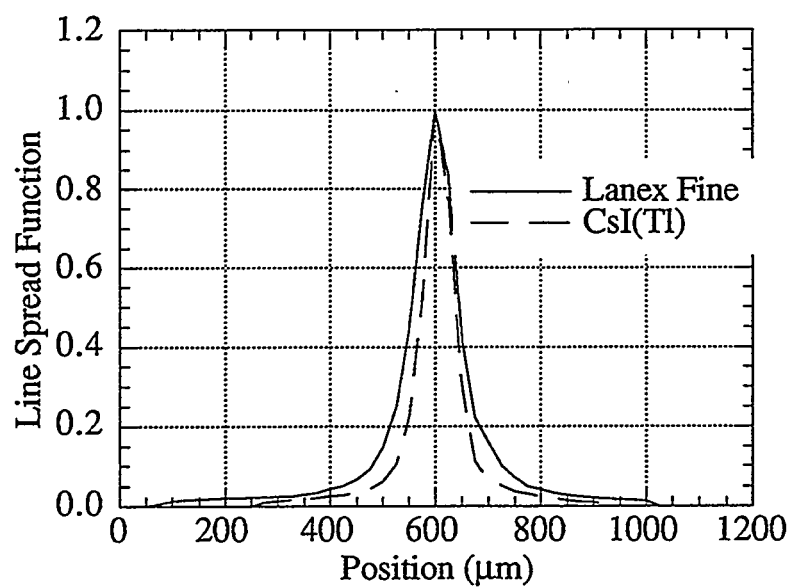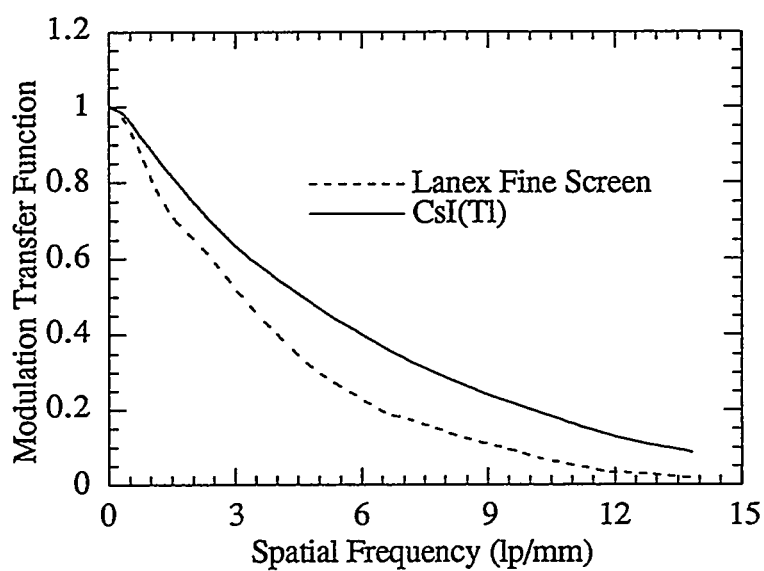
11

Fig.9 MIPs measurement (a) experimental setup;(b) pulse height distribution 1 MeV betas.

4.2 X-ray detection Spatial resolution

Measurements of the spatial resolution of the CsI(Tl) layer were carried out using a pulsed X-ray beam and a linear photosensor array. A narrow beam 20 μm wide was produced by collimating the X-rays through a Ta collimator slit which was aligned parallal to the photosensor strip. The photosensor array has 1024 strip pixels with pitch 25 μm and element width 20μm. A 4 mm thick fiber optics plate was cemented on the top of the array. The fiber plate can block the incoming X-ray photons which penetrate through the CsI layer, thus no signal will be generated by direct interaction between the X-rays and the photosensor. The very fine fibers(diameter less than 10 μm) ensured an identical light distribution between the output plate of the CsI layer and the window surface of the sensor array. The comparison of a FWHM of a CsI layer with thickness chosen to give the same light yield as Kodak Lanex Fine Intensifying screens used in medical radiography is given in Fig.10(a). The corresponding modulation transfer function of the CsI and the Lanex screen is shown in Fig.10(b). The CsI layer has a higher resolution than the Lanex screen at all spatial frequencies.
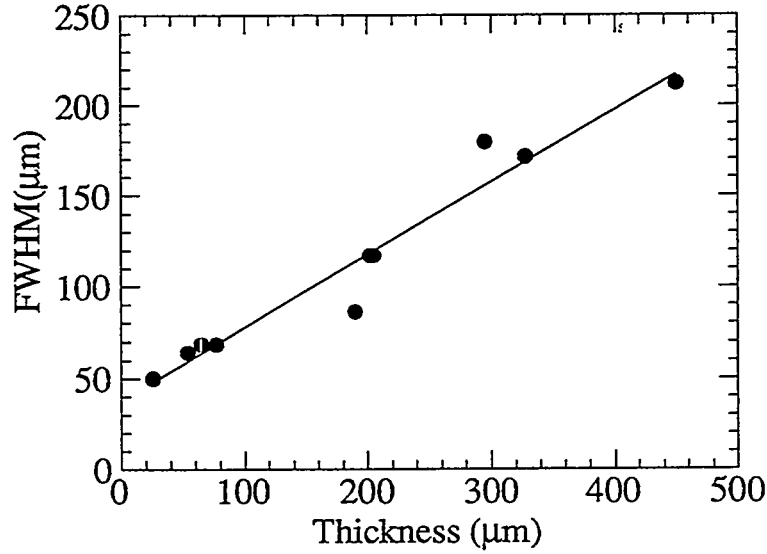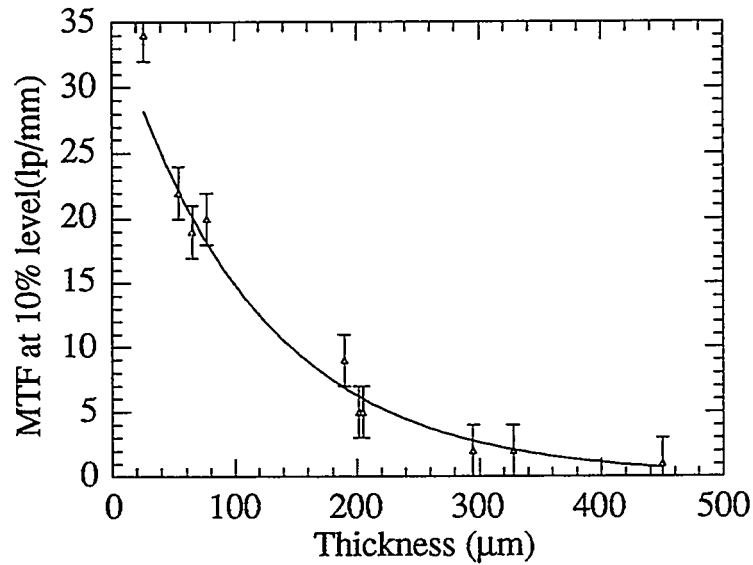
Fig.10 Spatial resolution measurement (a) line spread function of Kodak Lanex

Fine screen and evaporated CsI layer with same light emission at equal

X-ray flux;(b) The corresponding modulation transfer functions.

13

With increasing thickness of the scintillator, the X-ray absorption increases, the light output also increases, but the resolution decreases. Fig.11(a) and (b) show the spatial resolution dependency of CsI(Tl) layers on their thicknesses.

(a)

(b)

Fig.11 (a) the FWHM of various thickness CsI(Tl) layers; (b) the corresponding MTF.

5. Photoconductive gain

Primary photocurrent devices (such as a p-i-n diode under reverse bias) have unity optical gain and a fast response (order of ns) time. In constrast, secondary photocurrent structures, such as n-i-n diodes or p-i-n diodes under forward bias, exhibit high optical photoconductive gain determined by the ratio of the electron lifetime to transit time[22].

Fig.12(a) shows typical current-voltage characteristics of a single photoconductive element. The relatively large current due to electron and hole injection from the electrodes will degrade the light to dark sensitivity or signal to noise ratio due to the current shot noise. The shot noise can be reduced by using small area pixels; for a 100X100μm pixel with shaping time 1μs and gain of 4, the noise level is about 2300 electrons.
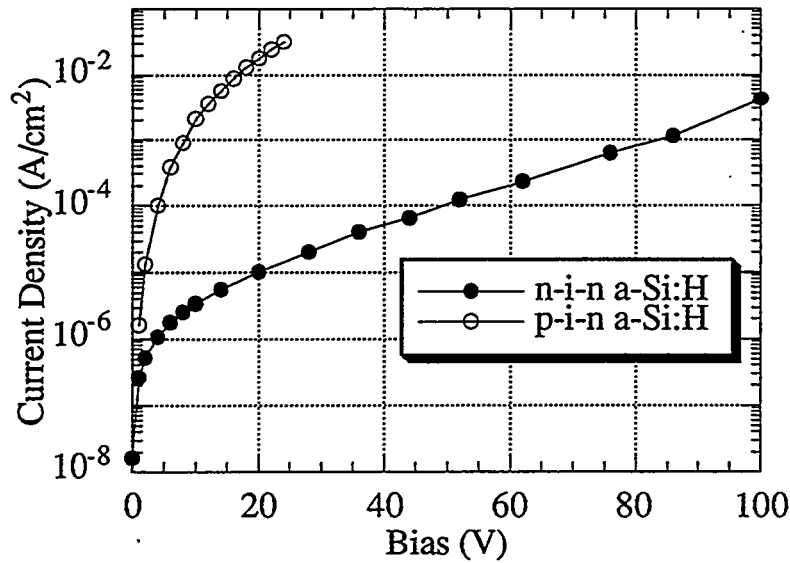
Fig.12(a) I-V characteristics of 14 μm thick n-i-n and p-i-n devices under forward bias.
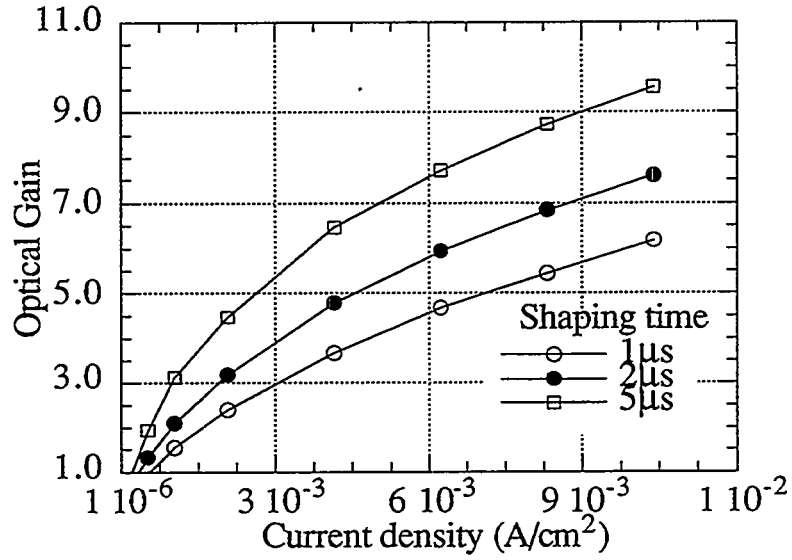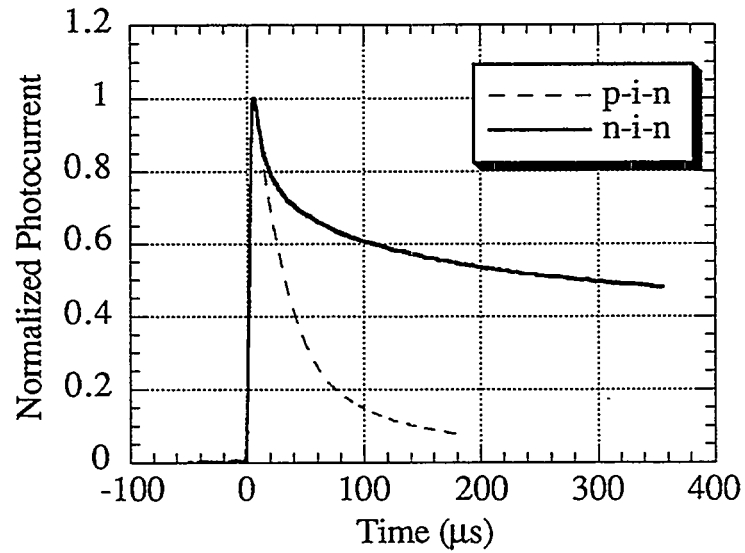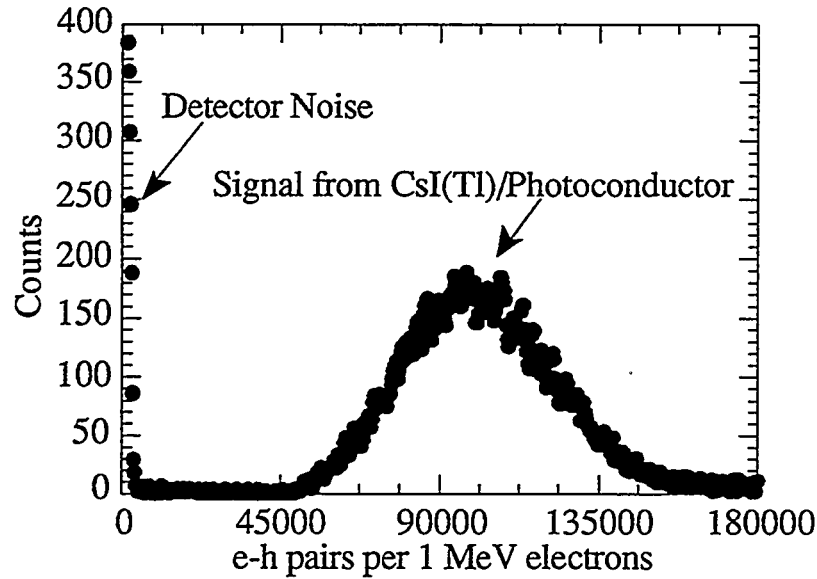
Fig.12 (b) Gains obtained fron a p-i-n device under forward bias with different shaping times;

Fig.12(b) shows optical gains obtained from a p-i-n 14 μm thick diode for different integrating time
The illumination source was a 665 nm LED emitting 200ns pulses. Fig.13(b) shows the measured pul
height spectrum from a Sr[90] source using the p-i-n device operated under forward bias with a gain or
coupled to the CsI(Tl) scintillator, using a shaping time of 1 μs.
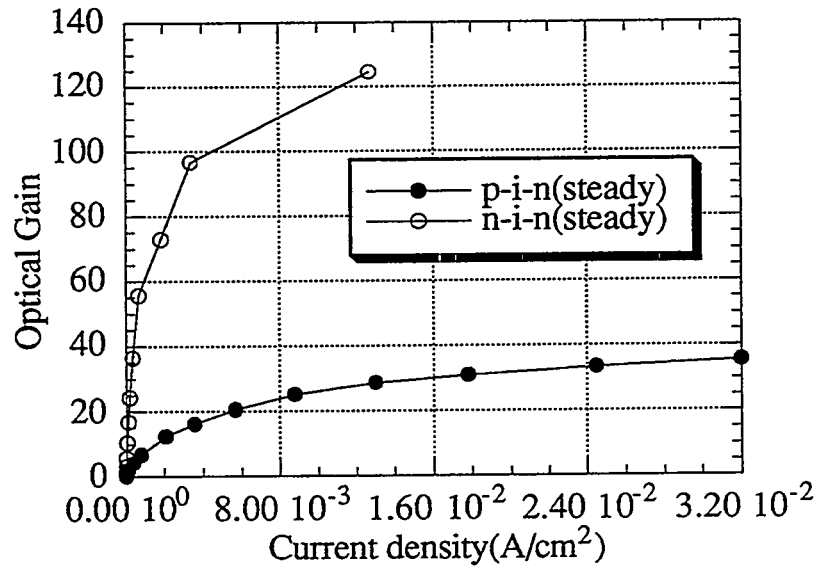

(a)

(b)

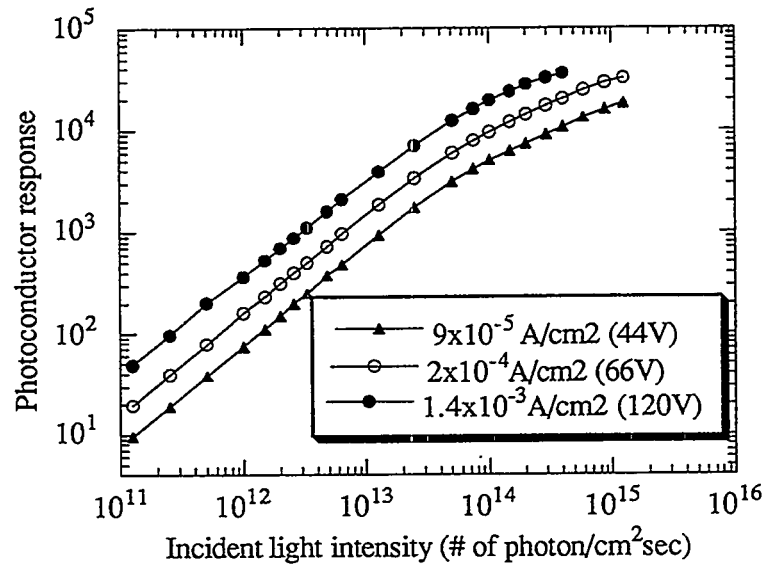Fig. 13(a) Photocurrent decay with time excited by a short light pulse.

(b) the Beta spectrum from a photoconductor coupled to a 900 μm CsI(Tl) layer

with 1 μs shaping time.

The signal from a-Si:H device operated as a photoconductor has long time decay components several ms long. By integrating the photoresponse with long enough time, or measuring a DC reponse, the photoconductive gain for the steady state can be obtained. For medical imaging where X-ray radiation exposures are typically 10milliseconds or longer, there is a difference between the integrated pulses from p-i-n and n-i-n devices. A n-i-n device exhibits a larger gain than the p-i-n one because hole injection through p-i junction increases the recombnation rate with the secondary electrons, and therefore reduces the optical gain. Fig.13(a) shows the responses of p-i-n and n-i-n devices to short light pulse ~200ns. The amplitues of the photocurrents of these two structures are very close in first 10μs, which result in the same optical gain for a short integrating time. However, the photocurrent of the p-i-n device decays faster than the n-i-n device after 10 μs, in the other word, secondary current of the n-i-n device lasts loner time, hence its optical gain for a long time integral is much higher than the p-i-n one as seen in Fig.13(a). Fig.14(a) shows the long term gain integrated over 10ms. Fig.14(b) shows data for the photon response of the photoconductor

17

as a function of high incident light intensity to simulate medical X-ray exposures. It is seen that the response increases as the 0.9 power of the incident light flux. Such a sublinearity is acceptable in many application including in medical imaging.

(a)

(b)

Fig.14 (a) Long term optical gains of n-i-n and p-i-n devices. (b) response of the photoconductor to incident light intensity.

6. Conclusion and discussion

The performances of a-Si:H p-i-n photodiodes coupled to CsI(Tl) scintillator for charged particle and X-ray detection have been measured. The ability to detect the minimum ionizing particles with S/N > 20 was demonstrated by using electrons with energies Ee>1.5 MeV from Sr^{90} source. For medical imaging, the evaporated CsI(Tl) layers exhibit superior spatial resolution to the Kodak commercial scintillators due to their internal columnar structure. For the same X-ray sensitivity as commercial scintillator screens, CsI(Tl) layers gave much large signals. Measurement of radiation resistance of the CsI(Tl) layer has shown that CsI(Tl) layers have long term stability under X-ray radiation, which is essential for medical imaging. a-Si:H n-i-n and p-i-n diodes can be operated as photoconductors with an increase of the light sensitivity. For short times pulses with shaping time less than 5 μs, p-i-n and n-i-n structures give the same optical gain. However, for long term integration ~ miliseconds, the n-i-n device has a factor of 3 higher optical gain than the p-i-n structure, due to longer secondary current decay from n-i-n device. A-Si:H diodes with photoconductive gain exhibit a good linenarity to incident light photon flux up to 10^{15}photon/cm^{2}sec with a power of 0.9 and is appropriate for medical imaging.

7. Acknowledgments

References

[1] R. A. Street,"Hydrogenated amorphous silicon", Cambridge university Press, p366 (1991).

[2] I. Holl et al., IEEE Trans. Nucl. Sci. vol. 35, No. 1, 1988, p. 105-109.

[3] T. Jing et al., IEEE Trans. Nucl. Sci. vol. 39, No. 5, 1992, p. 1195-1198.

[4] J. D. Joannopoulos et al., "The Physics of Hydrogenated Amorphous Silicon II," Springer-Verlag, 1984 p141.

[5] R. J. Schwartz et al., Tech. Dig. of the PVSEC-4, Sydney, p 607-613 (1989).

[6] A. Catalano et al., IEEE Trans. Electron Devices, Vol. 36, No.12, p2839-2842 (1989).

[7] C. van Berkel et al., J. Non-Crystalline Solids 164-166 p653-658 (1993)

[8] H. Ito et al., Mat. Res. Soc. Symp. Proc., Vol.95, p-437-444 (1987)

[9] H. Cho et al., IEEE Nuc. Sci., NS40, p323-327 (1993)

[10] M. F. Sakamoto et al., IEEE Trans. Comp., Hybr., Man. Tech., Vol. CHMT-7, N 4,p429-433 (1984).

[11] H. Mimura et al., Applied Surface Science Vol 48/49, p521-525 (1991).

[12] K. Rosan et al., IEEE Trans. Electron Devices, Vol. 36, No.12, p2923-2925 (1989).

[13] J. A. Shepherd et al., IEEE Trans. Nucl. Sci. Vol.40, No.4, p 413-416 (1993).

[14] T. Jing et al, IEEE Trans. Nucl. Sci. Vol.41, No.4, p 903-909 (1994).

[15] C. L. Melcher et al., Nucl. Instr. and Meth. A314, p212-214 (1992).

[16] C. W. E. van Eijk et al., Nucl. Instr. and Meth. A348, p546-550 (1994).

[17] V. Perez-Mendez et al., Nucl. Instr. and Meth. A260, p195-200 (1987).

[18] C. Bieler et al., Nucl. Instr. and Meth. vol. A234, p 435-442 (1985).

[19] S. Schlogl et al., Nucl. Instr. and Meth. vol. A242, p 89-94 (1985).

[20] M. Kobayashi et al., Nucl. Instr. and Meth. vol. A254, 1987, pp. 275-280.

[21] G. E. Giakoumakis, Applied Physics A-Solids and Surfaces, 1991, V52 N1:7-9

[22] J. I. Pankove, "Semiconductors and Semimetals," Vol. 21, Part B, Academic Press, Inc. 1984 p264.